

Physical and Dynamical Parameters of the Multiple System HD 222326

R. Ya. Zhuchkov¹, E. V. Malogolovets², Yu. Yu. Balega²,
I. F. Bikmaev¹, M. K. Kuznetsov³, and V. V. Orlov⁴

¹*Kazan State University, ul. Kremlevskaya 18, Kazan, 420008 Russia*

²*Special Astrophysical Observatory, Russian Academy of Sciences,
Nizhnii Arkhyz, Karachai-Cherkessian Republic, 357147 Russia*

³*Southern Federal University, ul. Bolshaya Sadovaya 105, Rostov-on-Don, 334006 Russia*

⁴*V.V. Sobolev Astronomical Institute, St. Petersburg State University,
Universitetskii pr. 28, Petrodvorets, 198504 Russia*

Received July 20, 2007; in final form, October 26, 2007

Abstract—We present the results of our study of the physical and dynamical parameters of the multiple system HD 222326. A new method for determining the individual radial velocities of components in wide binary and multiple systems in the case of small radial-velocity differences ($\Delta V_r \leq$ the FWHM for the line profiles) is suggested and tested for both model systems and the binary HD 10009. This testing yielded the component radial velocities $V_{r,1,2}$ for HD 10009, enabling us to derive the center-of mass velocity, V_γ , for the first time. We determined the radial velocities of the components of HD 222326 from high-resolution spectra, and refined the orbital parameters of the subsystems using speckle-interferometric observations. A combined spectroscopic and speckle interferometric analysis enabled us to find the positions of the components in the spectral type–luminosity diagram and to estimate their masses. It is likely that the components are all in various evolutionary stages after leaving the main sequence. We analyzed the dynamical evolution of the system using numerical modeling in the gravitational three-body problem and the known stability criteria for triple systems. The system is probably stable on time scales of at least 10^6 years. The presence of a fourth component in the system is also suggested.

PACS numbers: 97.80.Kq

DOI: 10.1134/S1063772908070044

1. INTRODUCTION

Binary and multiple stars are important for our understanding of the physical and dynamical evolution of the Galaxy. Between 70% and 90% of all stars in the Milky Way (and possibly in other galaxies as well) are members of binaries or multiple systems with a larger number of components (see, for instance, [1–3]).

According to current views, virtually all stars are formed in groups [4]. An attempt to restore the primordial multiplicity function was made by Goodwin and Kroupa [5], who claimed that stars are predominantly formed in binary and triple systems. Binary and multiple stars enable the direct determination of the fundamental parameters of these system: their masses, distances (when it is not possible to use the parallax method directly), and some characteristics of their components (from analyses of their tidal dynamical evolution, apsidal motion, etc.).

At the same time, studies of binary and multiple systems can encounter considerable difficulties, es-

pecially if it is not possible to obtain information for the components separately, so that studies are limited to photometry or spectroscopy of the system as a whole. The main, if not only, technique that can yield a complete set of physical parameters for the components of multiple systems is the synthetic-spectrum method, when a grid of component parameters is used to compute model atmospheres and then to construct a synthetic spectrum of the system that can be compared to observations. However, in this case, we have at least ten independent variables even for a two-component spectrum, and the number of parameters increases for systems of higher multiplicity. This is an ill-posed problem, and finding the solution is facilitated by reducing the number of free parameters step by step, using various methods to determine various parameters at all stages of the spectral reduction, before the actual modeling.

Among the parameters needed to begin the modeling are individual radial velocities of the compo-

nents, V_{ri} . While this is not difficult for close (or very wide) pairs, deriving V_{ri} is problematic for moderately wide systems (with orbital periods $500^d \leq P \leq 5000^y$), where we have only a combined spectrum and the lines cannot be separated. In such cases, the relative shifts of the components' lines are comparable to the widths of the lines and of the instrumental profile (and are often much smaller), making it impossible to estimate the shifts directly.

The current study is aimed at constructing a preliminary “phase portrait” of the triple system HD 222326, in preparation for applying the synthetic-spectrum method and reconstructing a complete set of physical parameters for the system. Since this is an ill-posed problem, it can only be solved iteratively and making use of various kinds of observations. The present paper presents the results of the first iteration.

The HD 222326 triple system is weakly hierarchic and, according to published data, is unstable on fairly short time scales ($\sim 10^6$ years) [6, 7]. This makes an analysis of the physical parameters of the system of special interest.

Basic information about the method used to determine V_{ri} from high-resolution spectra using the cross-correlation method, modified for the case of small relative line shifts, is presented in Section 2. This section also contains the results of testing the method using model binaries and the binary HD 10009. The application of the method to the HD 222326 triple system is described in Section 3. Section 4 presents the orbital solution derived for the system based on speckle interferometry with the 6-m telescope of the Special Astrophysical Observatory of the Russian Academy of Sciences (SAO). Section 5 presents the physical parameters of the system's components obtained by combining our speckle-interferometric and spectroscopic data. This section also contains the results of our analysis of the dynamical stability of the triple system. Section 6 summarizes the results of our study.

2. DETERMINING RADIAL VELOCITIES IN WIDE PAIRS

We applied the cross-correlation method to determine individual velocities V_{ri} in wide pairs with small relative line shifts and components with similar parameters ($\Delta m < 1.5^m$, $V_{rot1} \approx V_{rot2}$, where Δm is the different in the apparent magnitudes of the components and V_{roti} are their rotational velocities).

First, preliminary determined spectral types of the components are used to select spectra of standard stars for those spectral types taken with the same instrument. A model reference spectrum is formed by summing these with weights proportional to the

component brightnesses. Thus, we convert the two-dimensional radial-velocity grid to a one-dimensional grid, while simultaneously taking into account the spectra of both components (though they are very similar). This approach is valid for components with similar magnitudes, and is justified for $\Delta m < 0.5^m - 1^m$. If, however, $\Delta m \in (1^m, 1.5^m)$, we do not combine the reference spectra, and derive two auto-correlation functions in our analysis (see below), after which we determine their relative shift.

We then derive the cross-correlation function (e.g., see [8]) $CF(V_r)$, where V_r is the shift of the reference spectrum relative to the observed spectrum. Here we can write $CF(V_r) \simeq CF_1(V_{r1}) + CF_2(V_{r2})$, where, similarly, $CF_1(V_{r1})$, $CF_2(V_{r2})$ are the correlation functions of the reference spectrum relative to the spectra of the system's primary and secondary alone, whose arguments are the unknown radial velocities of each of the components.

Further, we derive the auto-correlation function of the reference spectrum, $ACF(V_r)$ (or two auto-correlation functions for each of the reference spectra separately, $ACF_{1,2}(V_r)$), and from this, the set of functions $CF(V_{r1}, V_{r2}) = ACF_1(V_{r1}) + ACF_2(V_{r2})$ for various radial-velocity shifts of each component.

Then, comparing the function $CF(V_r)$ earlier obtained to $CF(V_{r1}, V_{r2})$, we select the parameters V_{r1} , V_{r2} —the individual radial velocities of the system components that best fit the observations. Note that, since the radial-velocity difference is 10 km/s, the line shift between the components is only 0.17 Å, while the half-width of $CF(\Delta V_r)$ is about 0.2 Å.

This technique can also be applied to systems with more than two components if it is possible to find some part of the spectrum where the contributions of only two components dominate or to reduce the spectrum to the binary case in some other way.

To test this scheme, we prepared several combined spectra of model binaries for sets of radial-velocity differences between the components (which determine the appearance of the correlation-function profile, other parameters being the same) in the range $V_r = 0.5 - 10$ km/s (shifts of 0.01–0.15 Å between the spectra). We also varied the components' spectral types and the difference of their magnitudes, as well as the spectral resolution of the model spectra.

The individual spectra and composite spectrum for two model binaries are shown in Fig. 1, while the correlation functions $CF(V_r)$ and sets of functions $CF(V_{r1}, V_{r2})$ are displayed in Fig. 2. The parameters of the model binaries (spectral types, spectral resolution R , the signal-to-noise ratio S/N) can be found in the caption to Fig. 1.

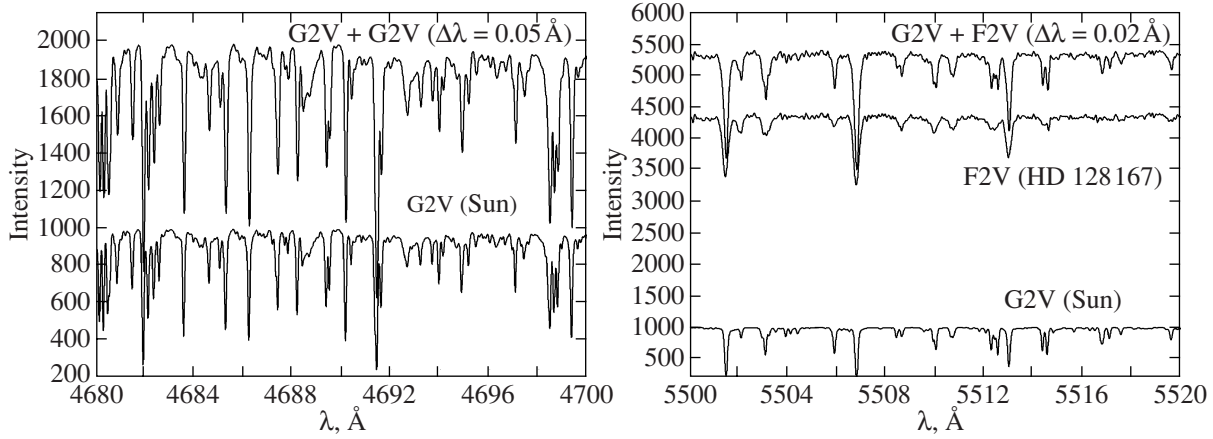


Fig. 1. Individual spectra of the standard stars and their sums, corresponding to the composite spectra of model binaries. The spectral types are indicated. The relative intensities are conserved. The shifts of the spectra for the model binary at $\lambda = 5500 \text{ \AA}$ are 0.05 \AA (2.7 km/s) ($G2V + G2V$, signal-to-noise ratio $S/N > 300$, $R = 500\,000$, spectrum taken from the solar atlas [9]; left) and 0.02 \AA (1.1 km/s) ($F2V + G2V$, $S/N \geq 100$, $R = 40\,000$, spectra taken with the Russian–Turkish telescope; right).

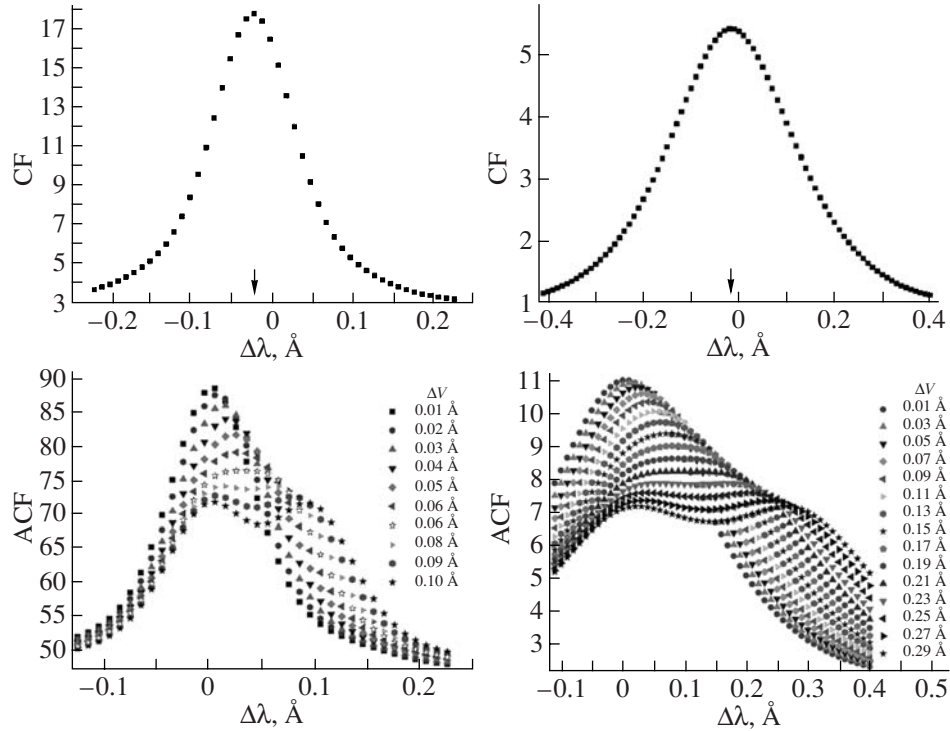


Fig. 2. The cross-correlation function (top; the position of the maximum is marked above the vertical axis) and the set of sums of the cross-correlation functions with various shifts (bottom). See text for details. The left panel shows the model $G2V + G2V$ binary, and the right panel the $F2V + G2V$ binary (see the spectra in Fig. 1). The radial velocities are expressed in \AA for $\lambda = 5500 \text{ \AA}$ (0.1 \AA corresponds to 0.55 km/s).

As a result, we were able to reproduce V_{ri} values close to those initially adopted for the model binaries. We estimated the uncertainty of our technique to be between 0.6 and 3 km/s , depending on R , S/N , $\Delta(V_{rot} \sin i)$ (the difference between the projections

of the axial-rotation rates on the line of sight, which considerably affect the line widths), and the agreement between the reference and observed spectra. The uncertainty is also influenced by how close the parameters of the standard stars are to those of the system's components. The uncertainty due to tem-

perature errors becomes less than 1 km/s if this agreement is within half a spectral type.

We also determined the limitations of the applicability of the algorithm: $\Delta m < 1.6^m$, $R \geq 40\,000$, and $S/N \geq 100$. We demonstrated that the uncertainties decrease with increasing R and S/N and with decreasing Δm and $\Delta(V_{rot} \sin i)$. The uncertainty reaches 3 km/s or more when $\Delta(V_{rot} \sin i) > (5-10)$ km/s.

After our tests using model binaries, we applied the technique to determine the component radial velocities for the relatively wide and well-studied speckle-interferometric and spectroscopic binary HD 10009 (with an orbital period of $P \approx 29$ years). We selected this object to test our algorithm because the orbit and physical parameters of the pair are well known, making it possible to predict the radial velocities (strictly speaking, their differences) for specified observation times. The binary's physical and orbital parameters are collected in Table 1.

We obtained spectra of HD 10009 on August 28 and 29, 2005 using the Coude echelle spectrograph of the 2-m Zeiss-2000 telescope at Peak Terskol [12]. The spectra have $S/N > 150$ and $R = 45\,000$. We used standards with spectral types F2V (HD 128167) and G2V (the Sun) as reference stars.

We then determined the individual velocities, $V_{r1,2}$, and V_γ , and calculated the ephemeris values using the “orbit” code [13]. Since V_γ was not known beforehand, we calculated only the ephemeris difference, $V_{r2} - V_{r1}$.

All these values are presented in Table 2. We can see that the radial-velocity difference for the components for the time of our observations was only 0.5 km/s. Given the small magnitude difference and the fact that, in this case, $V_{rA} = -V_{rB}$ (in the coordinate system of the binary's center of mass) with an accuracy of no worse than 0.05 km/s, we can assume that $V_{r,eff} = V_\gamma$ (cf. Section 3 for the definition of $V_{r,eff}$), at least within 0.05 km/s. Thus, the directly measured velocity will correspond to the gamma velocity of the system. V_γ was not determined for this system previously. We measured $V_{r,eff}$ using the classical cross-correlation method, comparing the observed and reference spectra.

The difference $V_{r2} - V_{r1}$ we determined coincided with the ephemeris value within 0.35 km/s (for the adopted $\sigma_V = 1$ km/s), testifying to the correct operation of the algorithm. Thus, we were able to directly determine V_{r1} , V_{r2} , and V_γ for the system HD 10009 for the first time. The radial velocity determined earlier, $V_{r,eff} = 47.5$ km/s, with the claimed uncertainty of 0.5 km/s [14], is in full agreement with our results.

Table 1. Parameters of the system HD 10009

Parameter	[10]	[11]	Adopted value
P , years	28.8 ± 0.77	—	28.8
T_0 , Bessel year	1989.92 ± 0.012	—	1989.92
a	$0.324'' \pm 0.005''$	—	0.324''
e	0.798 ± 0.007	—	0.798
Ω	$159.6^\circ \pm 0.73^\circ$	—	159.6°
ω	$251.6^\circ \pm 0.67^\circ$	—	251.6°
i	$96.6^\circ \pm 0.33^\circ$	—	96.6°
M_1, M_\odot	1.20	1.40	1.3
M_2, M_\odot	0.96	0.95	0.95
M_1/M_2	1.25	1.47	1.37
Sp ₁	F5V	F5	F5
Sp ₂	G	G3	G3

We determined $V_{r,eff}$ in several independent ways: through a cross-correlation of the entire spectrum with the reference spectrum, as well as by averaging the individual velocities for lines of heavy elements (Table 2). The difference between the methods is within 0.1 km/s.

Thus, our testing of the algorithm using both model and real binaries demonstrates its applicability within its claimed uncertainty. This approach can be used to analyze the component radial velocities for binaries when direct measurements of the radial-velocity differences are not possible.

The next section describes our application of this approach to the multiple system HD 222326.

3. RADIAL VELOCITIES OF THE COMPONENTS OF HD 222326

Further, we applied the technique to the multiple system HD 222326 (ADS 16904, HIP 116726, $\alpha_{2000} = 23^h 39^m 20.8^s$, $\delta_{2000} = +45^\circ 43' 12''$). This is a relatively bright object ($m_v = 7.63^m$), which is of interest primarily because a stability analysis based on earlier published parameters demonstrates the triple system to be dynamically unstable on times shorter than 10^6 years. It is very important to confirm (or disprove) and explain this result based on astrophysical data [6, 7].

In 2004–2006, we used the Coude echelle spectrometer of the Russian–Turkish 1.5-m telescope (RTT) to obtain a series of high-resolution ($R = 40\,000$) spectra of the system at wavelengths 4000 –

Table 2. Ephemeris and measured differences in the component radial velocities for HD 10009

Parameter	Ephemeris	Measured
V_γ , km/s (from lines)*	—	48.4 ± 0.1
V_γ , km/s (cross-correlation)*	—	48.34 ± 0.05
V_{r1} , km/s	$V_\gamma - 0.1$	48.1 ± 1.0
V_{r2} , km/s	$V_\gamma + 0.1$	48.7 ± 1.0
ΔV_{r2-1} , km/s	0.2	0.55 ± 1.0

* It is assumed that $V_\gamma = V_{r,eff}$ within the uncertainties (see text).

8000 Å with $S/N \approx 100$, which were then subject to a preliminary analysis. The RTT is located at an altitude of 2500 m at the Turkish National Observatory [15].

Taking into account the inclinations of the orbital planes, the previously published orbital periods for the system ($\sim 15^y$, 150^y) [16] give differences for the component velocities of no more than 5–8 km/s, so that most lines in the spectrum consist of two or three lines with small relative shifts. The profiles are never observed to be separated, and the relative contributions of each component to the combined profile differ from line to line. Therefore, the V_r value found from a simple cross-correlation will not correspond exactly to the radial velocity of one of the components or to the gamma velocity, V_γ . Instead, it represents a velocity close to the gamma velocity—the $V_{r,eff}$ velocity of the “effective photocenter” of the lines, which agrees V_γ within 5 km/s. For the given orbital periods, $V_{r,eff} = \text{const}$ to within 0.5 km/s during $\sim (3-5) \times 10^2$ days.

Note that Grenier et al. [17] reported possible radial-velocity variability for the earlier determined $V_r = -17.5$ km/s (they probably determined a value close to $V_{r,eff}$, since they did not plot a radial-velocity curve and the technique used to determine V_r was

Table 3. Radial velocities of components A and B of HD 222326 and the system’s $V_{r,eff}$

Date	$V_{r,eff}$, km/s	V_{r1} , km/s	V_{r2} , km/s
1999 [17]	−17.5 (var.)	—	—
2004.10.29	-1.3 ± 0.1	—	—
2004.10.30	-1.4 ± 0.1	2.8 ± 1.0	-5.6 ± 1.0
2005.09.19	-0.9 ± 0.2	3.4 ± 1.0	-5.2 ± 1.0
2005.12.20	-0.4 ± 0.1	2.4 ± 1.0	-3.2 ± 1.0
2006.07.12	-0.3 ± 0.2	—	—
2006.07.19	-0.1 ± 0.1	3.7 ± 1.0	-3.9 ± 1.0

the same as that applied for single stars). Table 3 presents all the available $V_{r,eff}$ values from our study and from [17]. We also give individual velocities for the two brighter components of the system, for which we first determined their spectral types, G0–G5, and estimated their rotation rates projected onto the line of sight, $V_{roti} < (5-8)$ km/s (cf. Section 5). We used G2V (the Sun) reference spectra for these components.

The third component of HD 222326 is fainter than either of the two brighter components by approximately 2^m in the red, which, combined with the absence of any strong lines of heavy elements and the high effective temperature ($T_{eff} > 15\,000$ K) (cf. Section 5) indicates that the spectrum at $\lambda > 6000$ Å includes contributions from only the two brighter components. Thus, we can determine V_{ri} for components A and B of the system using the technique described above. Figure 3 displays the correlation functions for the spectrum of HD 222326 taken on December 20, 2005.

However, our technique cannot be used to identify the particular star of a system that corresponds to the derived V_{ri} , in the case of two components with similar spectral types. Judging from the ephemeris radial velocities, the velocity we denote as V_{r1} corresponds to component A and V_{r2} to component B. This is true even if we admit the possible presence of a fourth component in the system (see below).

At the same time, the brightness of the third component, C, in the blue ($\lambda < 4000$ Å) is comparable to that of components A and B, and it seemed possible to determine V_{rC} after subtracting standard spectra for spectral types close to those of components A and B from the initial spectrum. However, this was not possible due to the characteristic features of HD 222326C (see Section 5)—the lines in the residual spectrum after the subtraction are very weak and have considerable half-widths, hindering a reliable velocity determination on their basis.

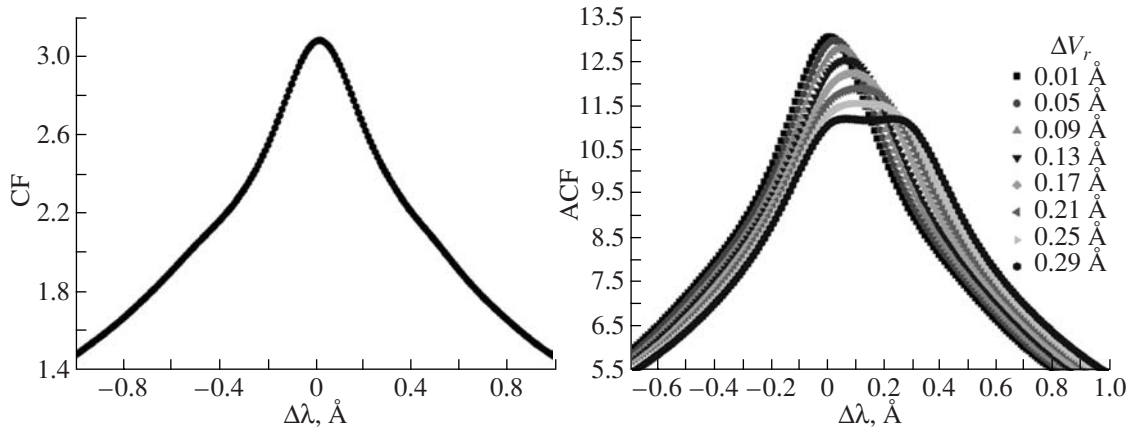


Fig. 3. Correlation function (left) and the set of sums of the auto-correlation functions with various shifts (right) for the spectrum of HD 222326 taken on December 20, 2005. See text for details. The radial velocities are expressed in \AA for $\lambda = 5500 \text{\AA}$ (0.1\AA corresponds to 0.55 km/s).

Table 3 shows that our results disagree with the data of [17]. This difference can be explained by actual variations of $V_{r,eff}$, if there the system contains a fourth stellar body with a relatively short period, $P \approx (10^2 - 10^3)$ days. A change by $\Delta V_{r,eff} \approx 16 \text{ km/s}$ is not possible for the existing configuration: given the inclination, this velocity exceeds the escape velocity for any component of the system. However, it may be that the difference is simply due to measurement errors, because the earlier radial velocities were determined from low-resolution spectra, and the actual uncertainty could be much higher than is claimed in [17] ($2 - 5 \text{ km/s}$).

At the same time, during the 20 months of our observations, we noted a systematic increase of $V_{r,eff}$ by $\approx 1 \text{ km/s}$, at the limit of detection for the given uncertainties. The monotonic character of this variation suggests that it is not a measurement error.

However, according to the system ephemeris we computed for the three-component model with the known orbital parameters, the change of V_{rB} (for component B, which has the highest rate of V_r variations) between October 2004 and July 2006 is $\approx 0.4 \text{ km/s}$ towards higher values, while the corresponding $\Delta V_{r,eff}$ should be at least half this value, or no more than 0.2 km/s .

The ephemeris radial-velocity difference for the components varies slightly, from $\Delta V_{rAB} = 1.8 \text{ km/s}$ in 2004 to $\Delta V_{rAB} = 2.1 \text{ km/s}$ in July, 2006. Even taking into account a scatter of about 1 km/s , our measurements indicate this quantity to be larger by $5 - 6 \text{ km/s}$.

Based on this result, we suggest that the observations tend to indicate the presence of a fourth stellar-mass component (D) with a relatively short orbital

period (several years) in one of the subsystems. In this case, the velocity will vary considerably for at least one of the three known components, also leading to variations of $V_{r,eff}$. If the period is $P < 10^y$, this fourth body cannot be directly detected, even by speckle interferometry.

Though none of the individual facts on their own provide a conclusive argument for the presence of the fourth component D, given the current accuracy of the observations, all of them together do suggest the presence of a fourth body. For this reason, it does not make sense to derive V_γ by comparing the ephemeris and observed velocities.

On the other hand, no signatures of an additional star are found in the integrated spectrum. This may mean that the fourth component has a spectral type close to those of the other components, or that it has a low luminosity and a substantial mass (one option is a white dwarf). Component D should be a companion of one of the two bright stars, HD 222326A or HD 222326B, since only such a configuration provides variations of $V_{r,eff}$ detected from the lines of the G-type component. At the same time, its existence near B would create a weakly hierarchic system B–C–D, whose stability would be doubtful. Thus, if component D does exist, it is probably in a subsystem with component A. In this case, the quadruple system has a “2 + 2” hierarchical structure.

4. ORBITAL PARAMETERS OF HD 222326

The orbit of the visual binary ADS 16904 AB = HD 222326, with a period of $P = 292$ years, was first calculated by Heintz [18] based on visual micrometer observations. Zulevic [19] improved the system’s orbit, deriving the refined orbital period $P = 238$ years. In 1986, speckle interferometry was

Table 4. Orbital parameters of HD 222326

Parameter	Inner orbit	Outer orbit
P , years	23.6 ± 0.8	341 ± 56
T_0 , Bessel year	1998.7 ± 0.3	1926 ± 13
a	$0.038'' \pm 0.002''$	$0.27'' \pm 0.04''$
e	0.21 ± 0.04	0.14 ± 0.10
Ω	$75^\circ \pm 94^\circ$	$29^\circ \pm 12^\circ$
ω	$27^\circ \pm 94^\circ$	$152^\circ \pm 23^\circ$
i	$164^\circ \pm 12^\circ$	$147^\circ \pm 9^\circ$
σ_θ	2.6°	3.4°
σ_ρ	$0.002''$	$0.02''$

used to detect the binarity of the brighter component, ADS 16904A [20]. A preliminary orbit for the interferometric subsystem was first calculated in [16] using the measurements of [20] and interferometric data acquired with the 6-m SAO telescope. This same paper contains a revision of the orbital solution for the outer subsystem, ADS 16904AB [16]. The orbital periods were found to be $P_{in} = 15$ years and $P_{out} = 151$ years. The authors noted that the estimated orbital periods could not be entirely accurate, because the orbit of the inner, interferometric subsystem was calculated from only five measurements, and the visual and interferometric data available for the outer subsystem were concentrated near apoastron. In 2005, Olevic and Cvetkovic [21] used all the existing observations to derive orbital elements for both the outer pair, ADS 16904AB = HD 222326(A–BC), and the inner, interferometric subsystem, ADS 16904Aab = HD 222326BC. The new orbital periods were longer than the estimates of [16] by a factor of two and by 30% for the inner and outer subsystems, respectively.

The additional speckle-interferometry data acquired with the 6-m telescope of the SAO enables us to refine the orbital parameters for the entire triple system. In addition to these speckle-interferometric measurements, we also used the interferometric data of [20], visual measurements from the Washington Catalog of Double Stars (<http://ad.usno.navy.mil/wds>), and data from the Hipparcos astrometric mission [22] to calculate the orbits. Preliminary orbital elements were estimated using the method of Monet [23], then refined using the differential-correction technique (see discussion in [24]).

According to the telescope aperture ratio, 4 : 6, we assumed for the speckle-interferometric measurements of [20] a weight of 0.7, equal to that for

the 6-m SAO interferometry. The weight for the Hipparcos measurement [22] (epoch 1991.25) is inversely proportional to the error in the component vector ($\sigma_\rho = 0.005''$). We assigned weights to the visual measurements according to the characteristic uncertainty of the method used ($\sigma_\rho \sim 0.01''$). We reduced the motion of component A to the center of mass of HD 222326BC using the component-mass ratio $q_{CB} = 0.45$, estimated from spectroscopic data and the measured magnitude difference. Table 4 presents the orbital elements, with their rms deviations, while Fig. 4 shows the apparent relative-orbit ellipses for the inner subsystem, HD 222326BC, and the outer subsystem, HD 222326(A–BC). Our orbital elements agree with those of Olevic and Cvetkovic [21].

Table 4 shows that, within the errors, the inner and outer orbits can be nearly coplanar, though this is not definitely so—given the uncertainties in the orbital elements, the mutual inclination of the orbital angular-momentum vectors could be as large as about 45° .

5. PHYSICAL PARAMETERS AND DYNAMIC STABILITY OF HD 222326

The spectral type of the system determined earlier, A2, with the components' spectral types A2V + A2V + F0V [25], does not agree with high-resolution spectra of the system (Fig. 5). The line-depth ratios in the available spectra are nearly solar, i.e. the two brightest components have spectral types $\sim G$. It was also found that the relative line width at a given wavelength, λ , for HD 222326 and the Sun, $\left(\frac{I_{HD}}{I_{Sun}}\right)_\lambda$, decreased with decreasing λ . For example, the mean ratios were $\left(\frac{I_{HD}}{I_{Sun}}\right)_{8700} = 0.77$, $\left(\frac{I_{HD}}{I_{Sun}}\right)_{5520} = 0.67$, and $\left(\frac{I_{HD}}{I_{Sun}}\right)_{4610} = 0.53$. Thus, the system's spectrum possesses a “blue” continuum with few (or no) lines and displays no lines typical of B–A stars (such as MgII 4481 Å, etc.). If we assume that the chemical abundances for the stars in the system are not drastically different (the principal components display nearly solar heavy-element abundances), this is possible only in the presence of the gravitational stratification of elements during the stars' contraction—i.e., “sinking” of metals. This phenomenon can be observed in final evolution stages, beginning with the “blue–white sequence” of the Hertzsprung–Russell diagram (luminosity class VIII), when, after the ejection of the envelope (and hence an effective temperature increase, because deeper and hotter layers are

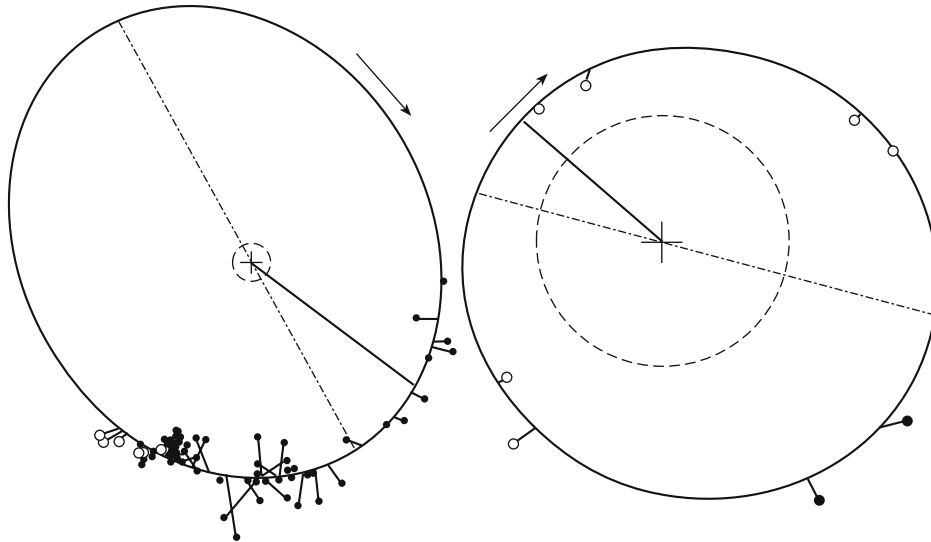


Fig. 4. Orbits of the subsystems in HD 222326. The left panel shows the outer orbit, HD 222326(A–BC), and the right panel the inner orbit, HD 222326(B–C). The radius of the dashed circle is $0.02''$, which corresponds to the diffraction limit for the 6-m SAO telescope in the visual. The open circles are 6-m observations, and the filled circles are observations of other authors. The solid line marks the position of periastron and the dot-dashed line the position of the line of nodes. The arrows show the direction of the relative orbital motion.

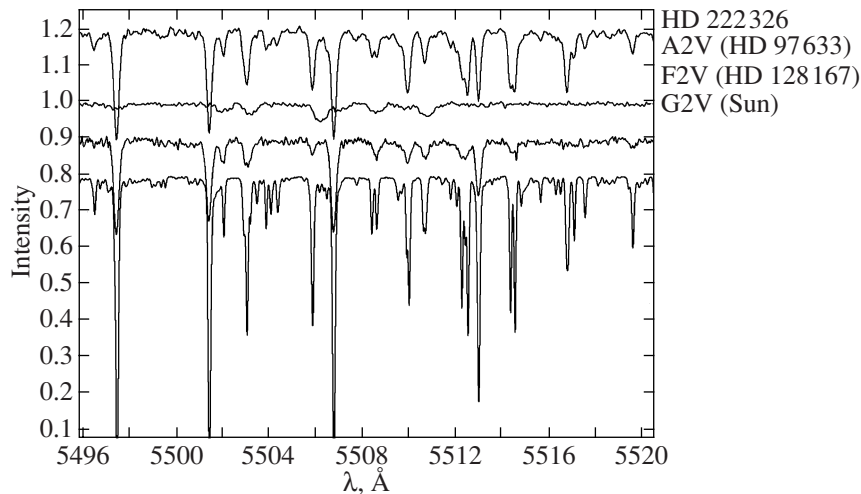


Fig. 5. Part of the spectrum of HD 222326 and of the spectra of standard stars of spectral types A2V, F2V, and G2V from the catalog [26] (the spectra are shifted along the vertical axis). All the spectra were taken with the Coude echelle spectrograph of the RTT ($R = 40\,000$, $S/N > 100$). It is obvious that HD 222326 cannot consist of an A2 star and an F0 star and have a combined spectral type A2[16].

observed), the contracting and cooling star moves downward in the spectral type–luminosity diagram.

Our analysis of the differential speckle photometry with the 6-m SAO telescope gave the results in Table 5, which confirm the evolutionary status of the third component. The brightest component is simultaneously the coolest, while the faintest component (C) has the highest temperature. All this means that the stars in the system cannot belong to the same luminosity class. At the same time, photometry of

HD 222326 as a whole yields an integrated spectral type that varies steadily with increasing wavelength. For the luminosity class III (see below), according to observations in the blue spectrum region, it is close to A5–F0 ($u - b = 0.27$), F0–F5 near the middle of the visible ($b - v = 0.43$) [27], F2–F6 in the near infrared ($v - i = 0.62$) [28], and F9–G6 in the far infrared ($v - j = 1.18$, $v - h = 1.50$, $v - k = 1.60$) [29]. Thus, the system becomes much “cooler” with increasing wavelength, also indicating the presence of an object

Table 5. Speckle photometry of HD 222326 and physical parameters of its components

Component	v	r	$(v-r)_{SI}$	$v-r$	T_{eff}, K	M_{vis}	M, M_{\odot}	Sp
	σ_v	σ_r	$\sigma_{(v-r)_{SI}}$	σ_{v-r}	$\sigma_{T_{eff}}, K$	$\sigma_{M_{vis}}$	σ_M, M_{\odot}	
1	2	3	4	5	6	7	8	9
A	8.53	7.95	0.00	0.58	5.7×10^3	0.93	1.2	G0III
	0.03	0.1		0.2	4×10^2	0.2	0.3	
B	8.66	8.34	-0.3	0.32	6.6×10^3	1.06	1.3	F3III
	0.04	0.1	0.2	0.2	4×10^2	0.2	0.3	
C	9.51	9.94	-1.0	-0.43	$< 2 \times 10^4$	1.91	0.7	sdO-BVIII
	0.05	0.1	0.2	0.3		0.2	0.4	

The component magnitudes are given assuming the integrated magnitudes of the system $v_{HD\ 222326} = 7.63^m$ [27], $r_{HD\ 222326} = 7.28^m$ (see text for discussion). The fourth column contains relative colors from speckle-interferometric measurements (the color index assumed for HD 222326A was $(v-r)_A = 0$). The colors in the fifth column are based on individual magnitudes of the components.

in the system that is *hot* and *compact* compared to the main components (for comparable radii, the integrated spectral type cannot change from A to G solely due to the temperature difference).

It is impossible to derive temperatures of the components from integrated photometry, but some constraints are possible. The hottest component (HD 222326C) cannot have a spectral type later than $\sim A6$ ($T_{eff}(C) > 8 \times 10^3$ K), and the coolest component (HD 222326A) cannot be hotter than $\sim G0$ ($T_{eff}(A) < 6 \times 10^3$ K). The temperature of HD 222326B must be in between these values, close to that of HD 222326A.

It is possible to improve the estimates, but this requires knowledge of the system's magnitudes in the v and r bands, which were those used for our differential speckle photometry on the SAO 6-m telescope. We were not able to find any published r magnitudes, but this value can be derived from photometry of the system in other bands in a wide (3650–22000 Å) wavelength range. Interpolating, we find $r = 7.28^m \pm 0.1^m$ (Fig. 6). The derived colors indicate that components A and B have spectral types no earlier than F0 (for any luminosity class), while the spectral type of component C is no later than A0; this is important for determining the evolutionary status of the components.

According to Hipparcos observations [30], the distance to the system is $r = 270$ pc. The distance modulus is then $m - M = -7.2^m$, yielding $M_v = 0.43^m$ as a “zeroth approximation” for the absolute magnitude of the system, which, in turn, yields the individual magnitudes $M_v(A) = 1.3^m$, $M_v(B) = 1.2^m$, $M_v(C) = 2.3^m$. The high luminosities of the two brighter components indicate that they have already

left the main sequence and are in the region of luminosity class III giants in the Hertzsprung–Russell diagram. On the contrary, the third component has a luminosity too low for its temperature (in terms of its position in the Hertzsprung–Russell diagram), providing a third piece of evidence that HD 222326C is a cooling evolved object.

Our derived colors yield for luminosity class III the component temperatures [31, 32] $T_{eff}(A) = 5.7 \times 10^3 \pm 400$ K, $T_{eff}(B) = 6.6 \times 10^3 \pm 400$ K, $T_{eff}(C) > 2 \times 10^4$ K. It is possible that the color index of HD 222326C is underestimated due to observational errors, and that its temperature must be determined spectroscopically.

We then obtain, for the corresponding temperature and luminosity data, the components masses $1.0 M_{\odot} < M_A < 1.5 M_{\odot}$, $1.0 M_{\odot} < M_B < 1.5 M_{\odot}$, $0.3 M_{\odot} < M_C < 1.1 M_{\odot}$, with the probable spectral-type combination G0III + F3III + sdO–BVIII.

The large uncertainties of the temperature and other parameters are the result of our simultaneous determination of many interrelated characteristics from observations that also have their errors. It is possible to check for consistency of our results with other observations, and to refine somewhat the parameters using the speckle-interferometric data. Let us determine the dynamic parallax of the system using the above estimates for the masses and orbital parameters. This method gives reliable results even for large mass uncertainties. This yields the distances $240 \text{ pc} < r < 340 \text{ pc}$ (for the inner subsystem) and $320 \text{ pc} < r < 360 \text{ pc}$ (for the outer subsystem). The Hipparcos distance [30] is $200 \text{ pc} < r < 410 \text{ pc}$. Thus, for the most probable value, $r = 330$ pc, the distance modulus is $m - M = -7.6^m$, leading to the refined

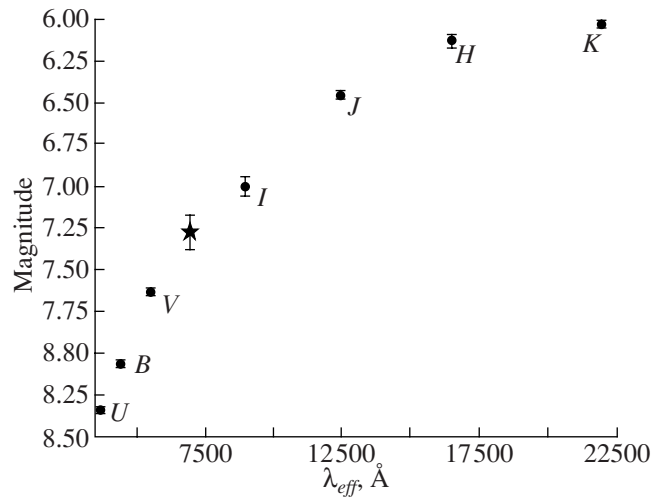


Fig. 6. Integrated photometry of HD 222326 in a wide spectral range, from [27–29]. The asterisk shows the interpolated r magnitude of the system.

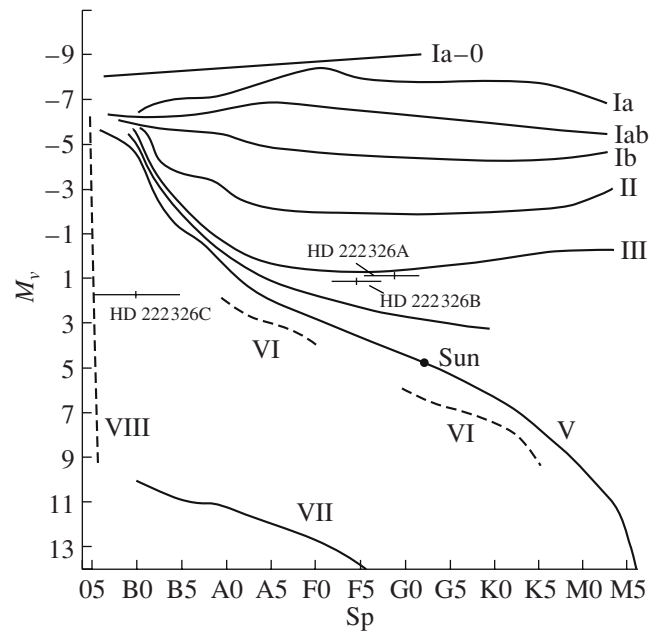


Fig. 7. Hertzsprung–Russell diagram with the positions of the three known components of HD 222326.

absolute magnitudes of the components $M_v(A) = 0.93^m$, $M_v(B) = 1.06^m$, $M_v(C) = 1.91^m$, with uncertainties not exceeding $\sigma_M \approx 0.2^m$.

The probable positions of the components in the Hertzsprung–Russell diagram are shown in Fig. 7.

We see that our results agree with the assumed spectral types and masses, and that the model for the system we have developed is self-consistent. Were our derived parameters in error, we would not find a full agreement simultaneously with all the available observations. Further improvement of the component

luminosities and other parameters of the system, possibly using our data and applying model atmospheres, will be the subject of a future study.

After our preliminary determination of the physical characteristics of the components and new determination of the system's orbital parameters, we should address the question of its stability. The methods used for our analysis are the same as those in our earlier publications [6, 7]. We checked the stability of the system through numerical modeling, as well as using nine stability criteria for triple systems: the tests

of Golubev [33, 34], Harrington [35, 36], Eggleton and Kiseleva [37], Mardling–Aarseth (two tests) [38, 39], Valtonen–Karttunen (three tests) [40, 41], and Tokovinin [42] (see [6, 7] for details).

Our modeling of the dynamical evolution demonstrated the system to be stable over the entire time covered by the model (10^6 years in the past and into the future) with a probability of 100%. Of 1001 Monte Carlo realizations (one corresponding to the observed parameters and with 1000 equally probable realizations constructed as described in [6, 7]), none showed instabilities for either the past or the future.

All the applied nine tests also indicated stability: for the vast majority of the realizations, the stability parameters in all the tests exceeded their critical values. This means that the HD 222326 system (at least for a configuration with the three known components) is far from the instability limit in the parameter phase space, and earlier conclusions that it was unstable were due to inaccurate orbital parameters reported in previous studies.

6. CONCLUSIONS

We have suggested a technique for determining the component radial velocities in wide stellar pairs and multiple systems from high-resolution spectra, based on the classical cross-correlation method. Our technique was successfully tested using model binaries with various parameters for their component spectra, and can be applied in future studies of binary and multiple systems.

We determined the radial velocities of the components of the binary HD 10009 and the velocity of its center of mass, as well as re-determined several parameters of the multiple system HD 222326 and derived the positions of its components in the spectral type–luminosity diagram. We also detected the probable existence of a fourth component (a white dwarf or low-luminosity star) in a pair with one of the system's bright components (most likely with component A). Our calculations were done using combined data from spectroscopy and speckle interferometry.

We have used new speckle-interferometric observations of HD 222326 to refine the orbital parameters of its subsystems. Modeling the evolution of the system for 10^6 years in the past and into the future indicates that it is dynamically stable.

ACKNOWLEDGMENTS

This study was partially supported by the Russian Foundation for Basic Research (project codes 05-02-17744-a and 07-02-91229-YaF) and the Program of Support for Leading Scientific Schools of the

Russian Federation (grants NSh-784.2006.2, NSh-4929.2006.2, and NSh-4224.2008.2). The authors are grateful to V.V. Shimanskii (Kazan University) for valuable discussions and assistance.

REFERENCES

1. W. D. Heintz, *Observatory* **89**, 147 (1969).
2. W. D. Heintz, *J. Roy. Astron. Soc. Canada* **63**, 275 (1969).
3. M. Mayor, S. Udry, J.-L. Halbwachs, and F. Arenou, in *IAU Symposium No. 200: The Formation of Binary Stars*, Ed. by H. Zinnecker and R. D. Mathieu (Astron. Soc. Pac., San Francisco, 2001), p. 45.
4. R. B. Larson, *IAU Symposium No. 200: The Formation of Binary Stars*, Ed. by H. Zinnecker and R. D. Mathieu (Astron. Soc. Pac., San Francisco, 2001), p. 45.
5. S. P. Goodwin and P. Kroupa, *Astron. Astrophys.* **439**, 565 (2005).
6. V. V. Orlov and R. Ya. Zhuchkov, *Astron. Zh.* **82**, 231 (2005) [*Astron. Rep.* **49**, 201 (2005)].
7. R. Ya. Zhuchkov and V. V. Orlov, *Astron. Zh.* **82**, 308 (2005) [*Astron. Rep.* **49**, 274 (2005)].
8. S. Zucker and T. Mazeh, *Astrophys. J.* **420**, 806 (1994).
9. R. L. Kurucz, I. Furenlid, J. Brault, et al., *Solar Flux Atlas from 296 to 1300 nm* (National Solar Observatory, Sunspot, New Mexico, 1984), Vol. 1.
10. D. Pourbaix, *Astron. Astrophys., Suppl. Ser.* **145**, 215 (2000).
11. I. I. Balega, Y. Y. Balega, K.-H. Hofmann, et al., *Astron. Astrophys.* **385**, 87 (2002).
12. F. A. Musaev, G. A. Galazutdinov, A. V. Sergeev, et al., *Kinematika Fiz. Nebesnykh Tel* **15**, 282 (1999) [*Kinematics Phys. Celest. Bodies* **15**, 216 (1999)].
13. A. Tokovinin, *Astron. Soc. Pac. Conf. Ser.* **32**, 573 (1992).
14. B. Nordstroem, M. Mayor, J. Andersen, et al., *Astron. Astrophys.* **418**, 989 (2004).
15. I. F. Bikmaev and N. A. Sakhbullin, in *Methods of Spectroscopy in Modern Astrophysics*, Ed. by L. I. Mashonkina and M. E. Sachkov (Yanus-K, Moscow, 2007), p. 26 [in Russian].
16. I. I. Balega, Yu. Yu. Balega, K. Kh. Khofmann, et al., *Pis'ma Astron. Zh.* **25**, 910 (1999) [*Astron. Lett.* **25**, 797 (1999)].
17. S. Grenier, M.-O. Baylac, L. Rolland, et al., *Astron. Astrophys., Suppl. Ser.* **137**, 451 (1999).
18. W. D. Heintz, *Veröff. Sternw. München* **7**, 34 (1967).
19. D. J. Zulevic, *Bull. Astron. Obs. Beograd* **150**, 117 (1994).
20. H. A. McAlister, W. I. Hartkopf, and O. G. Franz, *Astron. J.* **99**, 965 (1990).
21. D. Olevic and Z. Cvetkovic, *Serbian Astron. J.* **170**, 65 (2005).
22. M. A. C. Perryman, *The Hipparcos and Tycho Catalogues*, Europ. Space Agency Sci. Publ., SP-1200 (ESA, ESA Publ. Division, 1997).
23. D. G. Monet, *Astrophys. J.* **234**, 275 (1979).

24. T. Forveille, J.-L. Beuzit, X. Delfosse, et al., *Astron. Astrophys.* **351**, 619 (1999).
25. A. A. Tokovinin, *Astron. Astrophys., Suppl. Ser.* **124**, 75 (1997).
26. B. Garcia, *Bull. Inform. CDS* **36**, 27 (1989).
27. T. Oja, *Astron. Astrophys., Suppl. Ser.* **65**, 405 (1986).
28. T. F. Droege, M. W. Richmond, and M. Sallman, *Publ. Astron. Soc. Pac.* **118**, 1666 (2006).
29. R. M. Cutri, M. F. Skrutskie, S. Van Dyk, et al., *CDS/ADC Collection of Electronic Catalogues*, Vol. 2246 (2003).
30. M. A. C. Perryman, L. Lindegren, J. Kovalevsky, et al., *Astron. Astrophys.* **323**, 49 (1997).
31. *Allen's Astrophysical Quantities*, Ed. by A. N. Cox (Springer, Berlin, 2000).
32. M. V. Zombeck, *Handbook of Space Astronomy and Astrophysics*, 2nd ed. (Cambridge Univ. Press, Cambridge, 1990).
33. V. G. Golubev, *Dokl. Akad. Nauk SSSR* **174**, 767 (1967) [*Sov. Phys. Dokl.* **12**, 529 (1967)].
34. V. G. Golubev, *Dokl. Akad. Nauk SSSR* **180**, 308 (1968) [*Sov. Phys. Dokl.* **13**, 373 (1968)].
35. R. S. Harrington, *Celest. Mech.* **6**, 322 (1972).
36. R. S. Harrington, *Astron. J.* **82**, 753 (1977).
37. P. Eggleton and L. Kiseleva, *Astrophys. J.* **455**, 640 (1995).
38. R.-M. Mardling and S. J. Aarseth, in *The Dynamics of Small Bodies in the Solar System, a Major Key to Solar System Studies*, Ed. B. A. Steves and A. E. Roy (Kluwer, Dordrecht, 1999), p. 385.
39. S. J. Aarseth, *Gravitational N-body Simulations. Tools and Algorithms* (Cambridge Univ. Press, Cambridge, 2003).
40. M. Valtonen and H. Karttunen, *Three-Body Problem* (Cambridge Univ. Press, Cambridge, 2006).
41. M. Valtonen, private communication (2007).
42. A. A. Tokovinin, *Rev. Mex. Astron. Astrofis. Ser. Conf.* **21**, 7 (2004).

Translated by N. Samus'